Desalination and Water Treatment
www.deswater.com
doi: 10.5004/dwt.2022.28002

247 (2022) 121–131
January

Preparation, performance and mechanisms of glass pumice for Pb^{2+} removal from storm water runoff

Menglin Ba[a], Wanli Hou[b], Yu Cai[a], Jianghua Yu[a,*]

[a]*Collaborative Innovation Center of Atmospheric Environment and Equipment Technology, Jiangsu Key Laboratory of Atmospheric Environment Monitoring and Pollution Control, School of Environmental Science and Engineering, Nanjing University of Information Science & Technology, Nanjing 210044, China, Tel. 18751906939; email: yujh@nuist.edu.cn (J. Yu), Tel. 15736755895; email: 20191213002@nuist.edu.cn (M. Ba), Tel. 18751905195; email: 1148353956@qq.com (Y. Cai)*
[b]*Key Laboratory of Marine Environmental Science and Ecology of Ministry of Education, College of Environmental Science and Engineering, Ocean University of China, Qingdao 266100, China, Tel. 18303630900; email: 946515513@qq.com (W. Hou)*

Received 6 July 2021; Accepted 18 November 2021

ABSTRACT

The emerging concern of heavy metal pollution derived from storm water runoff has triggered a demand for effective heavy metal adsorbents. A novel adsorption material based on waste glass and cement blocks found in construction waste was developed, which showed the feasibility of its application in environmental adsorption materials. The preparation conditions of glass pumice were studied, and scanning electron microscopy, Brunauer–Emmett–Teller and Fourier transform infrared spectroscopy were used to analyze physical characteristics. The results showed that the glass pumice was prepared successfully when the ratio of glass powder/cement block/boric acid/calcium carbonate was 10:12:2.5:3 and the firing temperature at 1,000°C. Batch adsorption experiments were conducted to investigate its adsorption performance. Adsorption kinetics and adsorption isotherms were investigated to reveal the adsorption mechanisms. The results showed that the maximum adsorption capacity was 34 μg g^{-1} and the maximum removal efficiency reached 90% under pH 6.0, Pb^{2+} 0.5 mg L^{-1} and temperature at 25°C, which matched well with the second-order kinetics model and the Langmuir model.

Keywords: Construction waste; Glass pumice; Heavy metal; Adsorption performance

1. Introduction

Urban non-point source pollution represented by storm water runoff is difficult to be intensively treated due to its wide range of pollution and its variety of pollutants. Many studies had focused on heavy metal pollution caused by rainwater runoff and subsequent drainage overflow. Surface dust and suspended particles in the atmosphere aggravated the heavy metal pollution of surface runoff during rainfall [1–3]. Heavy metals exist in the water in the form of ions, and then enter human bodies, in which Pb^{2+} is one of the most toxic ions. High concentration of lead can cause death, while low concentration can damage the human nervous system, kidneys and other organs [4]. Thus, the removal of heavy metal from storm water runoff has become a crucial issue for water environment.

At present, heavy metal wastewater treatment technologies mainly include membrane separation, chemical precipitation, electrolysis, biological flocculation and adsorption, and also other methods [5,6]. The adsorption method has a broader application prospect because of its

* Corresponding author.

high adsorption efficiency, low cost, convenient operation, less sludge production and repeated use [7,8]. Several adsorbents have been used for the removal of lead. Sekar et al. [9] studied the adsorption performance of activated carbon for the heavy metal ions of lead, cadmium and copper. Natural zeolite was also used for the removal of lead [10]. Wu and Li [11] studied the mechanism of lead biosorption by *Phanerochaete chrysosporium*. Common adsorbents such as activated carbon [12] and zeolite [13] are restricted in widely use due to its high cost and secondary pollution problems. Hence, the selection of an environmentally friendly, cheap, sustainable and easy-to-obtain adsorbent is particularly necessary.

On the other hand, a large volume of construction waste was produced during rapid urbanization, such as demolition bricks, glass, cement blocks, concrete steel and soil. The characteristics of construction waste were large volume and rapid produce rate [14]. Not only did it occupy considerable amounts of space, but it also polluted the environment when it stored in piles for longtime, which caused negative environment effects [15]. At present, construction waste in China was mainly addressed by traditional landfill, direct utilization and recycling [16]. Since traditional landfill consumed a lot of land, and direct utilization cannot achieve full utilization, recycling had became a frequently-used treatment method. However, relevant data showed that the reuse rate was still less than 5% [17]. While common resource utilization methods of construction waste included the preparation of construction aggregates, mortar, concrete and ecological roofs [18], studies on using construction waste for adsorption were rare. Nevertheless, preparing adsorbent from construction waste has a great potential to become a substitute with high adsorption performance and low-cost.

This work aimed to produce a novel adsorbent based on construction waste, and then to analyze its adsorption performance. Glass pumice is a kind of porous lightweight inorganic material. It has numerous bubbles and micropores on its surface and in its interior, a large specific surface area and many adsorption sites, it is clear found its good mechanical strength, high compressive strength and good stability [19], thus it can be used as a novel adsorbent for further research. This work developed a novel adsorption material innovatively which used cement block and waste glass as raw materials, and applied it to the adsorption of heavy metal ions in surface runoff, with the aim of providing an applicable technology for urban non-point source pollution control and urban solid waste recycling.

2. Materials and methods

2.1. Preparation of glass pumice

The waste glass and cement blocks were collected from a nearby building demolition site. These were cleaned with distilled water several times to remove the dust and impurities from the surface, and then the materials were dried in an electro-thermostatic blast oven for 24 h at 105°C. The waste glass and cement block were crushed by high-speed pulverizer and 1~1.18 mm powder materials were selected as the prepared samples. Mix the glass powder and cement block powder that had been crushed and sieved in different proportions, then add moderate amounts of boric acid and calcium carbonate. Next, the material was calcined by muffle furnace at a high temperature, to conclude the preparation of the glass pumice. (Fig. 1 for a visual representation of the glass pumice preparation process).

2.2. Experimental chemicals

The sodium hydroxide (GR) was obtained from Shanghai Macklin Biochemical Co., Ltd., (China) Calcium carbonate (AR), boric acid (AR), hydrochloric acid (GR) was purchased from Sinopharm Chemical Reagent Co., Ltd., (China). Heavy metal solution of Pb were prepared from the Pb standard solution (GSB 04-1742-2004) which was purchased from Guobiao (Beijing) Testing & Certification Co., Ltd., (China). All chemicals were use as received, unless otherwise stated.

2.3. Experimental setup for preparation condition

The glass pumice was prepared by using glass powder, cement block powder, boric acid and calcium carbonate. The optimum matching condition was determined by controlling the proportions of boric acid, calcium carbonate and cement block powder. Because these proportions and the firing temperature would affect the compressive strength and preparation of glass pumice directly. Four experimental groups were set to discuss the influence of proportions of raw materials and the firing temperature on compressive strength and adsorption performance of the glass pumice. Therefore, different proportions of boric acid, calcium carbonate and cement block powder were mixed with glass powder. Next, the mixed sample was dried in an electro-thermostatic blast oven at 105°C for 24 h to remove moisture, and then placed into the muffle furnace for firing. The heating method adopted direct heating instead of indirect heating, as indirect heating method consumed more energy compared to direct heating. The mixed sample was fired with a heating rate of 10°C min^{-1}, holding the temperature at 1,000°C for 2 h. The fired sample was cooled down at room temperature and stored in crucibles. The whole process of preparing glass pumice is shown in Fig. 2. The details of experimental conditions are listed in Table 1.

2.4. Adsorption experiments setup

The adsorption was conducted in simulated heavy metal solution in this study. Put glass pumice into 100 mL plastic centrifuge tubes with 50 mL heavy metal solution (National Standard Sample GSB 04-1742-2004 Lead Single Element Standard Solution). To study its adsorption performance, 0.6 g glass pumice was placed into heavy metal solution (Pb^{2+} 0.5 mg L^{-1}) with pH 6. Then shake them in thermostatic oscillator at a speed of 120 rpm with a constant temperature of 25°C, finally the solution was removed at following times: 5 min, 10 min, 15 min, 30 min, 45 min, 60 min, 2 h, 4 h, 8 h, 12 h, 16 h, 20 h and 24 h. After the step of shake, an inductively coupled plasma optical emission spectrometer (ICP-OES) was used to determine Pb^{2+} concentration in solution that filtered through 0.45 μm filter membrane.

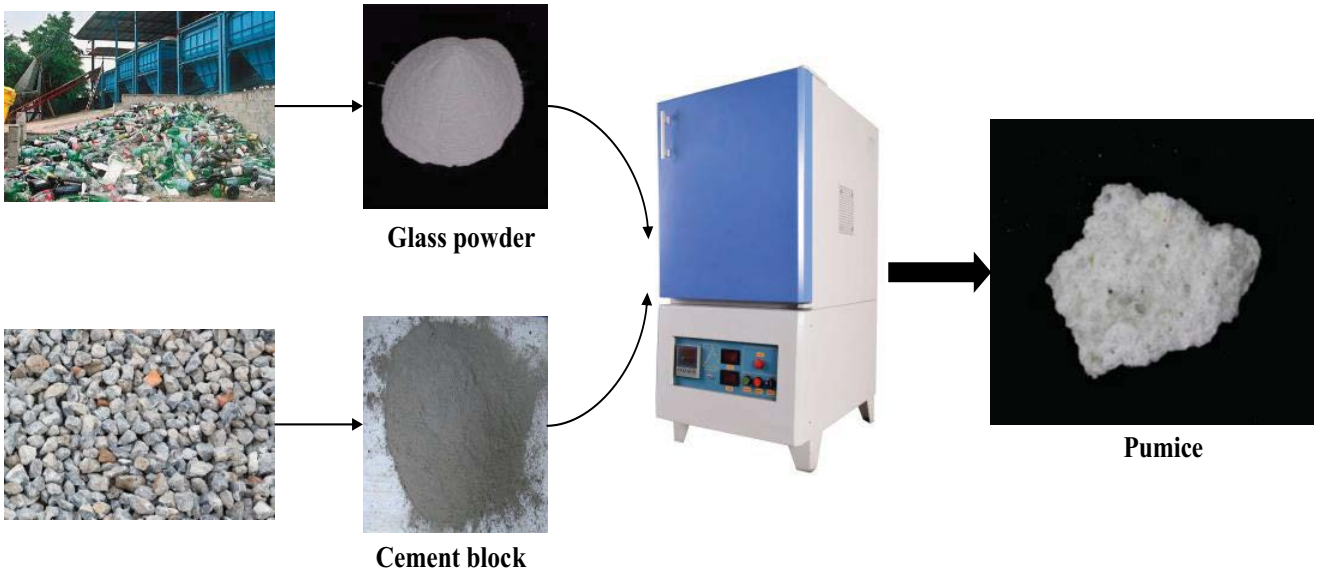

Fig. 1. Visual representation of the glass pumice preparation process.

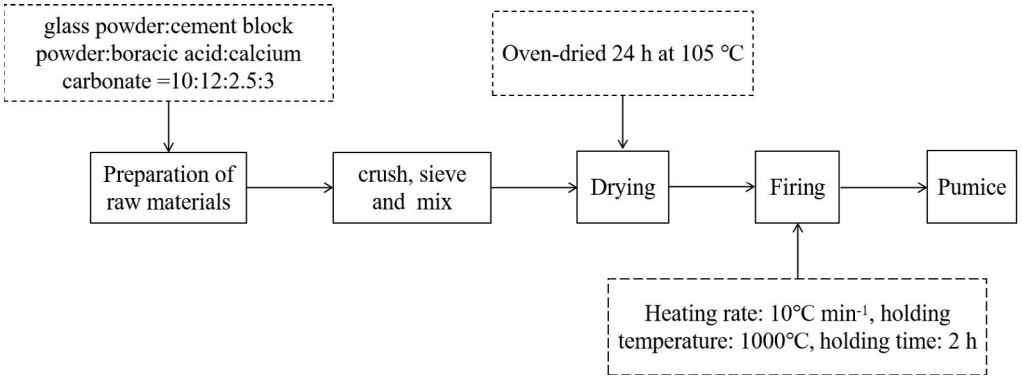

Fig. 2. The whole process of preparing glass pumice.

Table 1
Experimental conditions of preparing glass pumice

Experimental groups	(a)	(b)	(c)	(d)
Boric acid (g)	1, 1.5, 2, 2.5, 3, 3.5, 4, 4.5, 5	3	3	3
Calcium carbonate (g)	2.5	1, 1.5, 2, 2.5, 3, 3.5, 4, 4.5, 5	2.5	2.5
Cement block proportion (g)	12	12	6, 7, 8, 9, 10, 11, 12, 13, 14, 15	12
Firing temperature (°C)	1,000°C	1,000°C	1,000°C	900°C, 950°C, 1,000°C, 1,050°C, 1,100°C, 1,200°C, 1,300°C

To get its adsorption isotherms, the heavy metal solution with Pb^{2+} concentration was changed from 0 to 5 mg L^{-1}. Other conditions were similar to the above. Each sample was measured three times and the average value was analyzed, the repeatability (n) and the standard deviation (SD) of experiments were marked in the table and the figure.

2.5. Analysis methods

The microstructure of glass pumice was determined by scanning electron microscopy (SEM) with different magnifications to evaluate its physical properties; the Brunauer–Emmett–Teller (BET) was used to measure its specific

surface area, pore volume and pore size of the glass pumice; the Fourier transform infrared spectroscopy (FTIR) spectra for the glass pumice were performed with wavenumber from 400 to 4,000 cm^{-1}; and the energy-dispersive X-ray spectroscopy (EDS) was used to analyze the elemental composition of the glass pumice. Pb^{2+} concentration of heavy metal solution was measured by ICP-OES in the adsorption experiment.

2.6. Data analysis

2.6.1. Adsorption capacity

In this study, the adsorption efficiency of the glass pumice at equilibrium period was calculated by Eq. (1) and the adsorption capacity of the glass pumice at equilibrium period was calculated by Eq. (2):

$$\eta = \left(\frac{C_0 - C_e}{C_e} \right) \tag{1}$$

$$q_e = \frac{\left(C_0 - C_e\right)v}{m} \tag{2}$$

where η is the adsorption efficiency of the glass pumice at equilibrium period; C_0 and C_e are the initial and equilibrium concentrations of Pb^{2+} in the adsorbents respectively (mg L^{-1}); q_e is the amount of Pb^{2+} adsorbed by the glass pumice at equilibrium time (μg g^{-1}); v is the heavy metal solution volume (L); and m is the mass of glass pumice (g).

2.6.2. Adsorption kinetics

In order to explain the adsorption kinetics of Pb^{2+} by glass pumice, the first-order kinetics model and the second-order kinetics model were used to illuminate the adsorption process [20]. The first-order kinetics model is controlled by the diffusion of Pb^{2+} from the solution to the surface of the glass pumice while the second-kinetics is controlled by chemical adsorption. Eq. (3) represents the first-order and Eq. (4) represents the second-order:

$$\ln\left(q_e - q_t\right) = \ln q_e - k_1 t \tag{3}$$

$$\frac{t}{q_t} = \frac{1}{k_2 q_e^{\,2}} + \frac{1}{q_e} t \tag{4}$$

where q_e is the adsorption capacity fitting value of the glass pumice at equilibrium period (μg g^{-1}); q_t is the adsorption amount at t time (μg g^{-1}); k_1 is the first-order adsorption rate constant (h^{-1}) and k_2 is the second-adsorption rate constant (h^{-1}).

2.6.3. Adsorption isotherms

The adsorption isotherms were fitted by Freundlich model and Langmuir model. The Langmuir model assumes that the adsorption is a single-layer adsorption, and the adsorbate is uniformly adsorbed on the surface of the adsorbent [21], while the Freundlich model assumes that the adsorption is a multi-molecular layer adsorption [22]. Eq. (5) represented the Freundlich model and Eq. (6) represented the Langmuir model:

$$q_e = K_F C_e^n \tag{5}$$

$$q_e = \frac{q_{\max} K_L C_e}{1 + K_L C_e} \tag{6}$$

where q_e is the adsorption capacity fitting value of the glass pumice at equilibrium period (μg g^{-1}); $q_{\max}$ indicates the maximum adsorption (μg g^{-1}); K_L indicates the Langmuir relative binding energy of the glass pumice (L mg^{-1}); K_F and n represent the Freundlich relative adsorption capacity and adsorption intensity of glass pumice respectively (L mg^{-1}); K_F is indicative of the adsorption capacity of the adsorbent and n is a measure that used to verify types of adsorption; C_e is the equilibrium concentration of Pb^{2+} remaining in heavy metal solution (mg L^{-1}).

Further, the essential characteristics of the Langmuir isotherm can be descried by a separation factor R_L: which is defined by Eq. (7):

$$R_L = \frac{1}{\left(1 + bC_e\right)} \tag{7}$$

where C_e is the initial concentration of heavy metal solution (mg L^{-1}) and b is the Langmuir constant (g L^{-1}). The value of separation factor R_L, indicates the nature of the adsorption process as given below:

R_L value	Nature of adsorption process
$R_L > 1$	Unfavorable
$R_L = 1$	Linear
$0 < R_L < 1$	Favorable
$R_L = 0$	Irreversible

3. Results and discussion

3.1. Optimization of glass pumice preparation conditions

The effect of raw material proportion and firing temperature on glass pumice compressive strength is shown in Fig. 3. It represented the process of optimizing the preparation conditions, and the results demonstrated that the raw material proportion and firing temperature would affect the compressive strength directly. Besides, comparing the physical properties of prepared glass pumice with similar products, the different results are listed in Table 2.

3.1.1. Effect of calcium carbonate proportion

As for calcium carbonate, with the increase of calcium carbonate proportion, the compressive strength of glass pumice showed a trend of first increasing and then decreasing. The maximum compressive strength was reached when the proportion was 2.5 in Fig. 3a. However, as the proportion of calcium carbonate continued to increase, the compressive strength of glass pumice then decreased obviously. Moreover, calcium carbonate, as a foaming agent, played

Table 2
Comparisons of the physical properties of glass pumice and similar products

Name	Material source	Appearance	Service life	Porosity (%)	Surface area	Compressive strength (MPa)
Glass pumice	Artificial	Porous particles	Long time	50–65	Big	1–13
Ceramsite	Artificial	Oval sphere	Short time	55–75	Medium	10
Vermiculite	Natural	Layered	Short time	81–93	Big	1–1.5
Diatomite	Natural	Microporous	Short time	90–92	Big	1–7

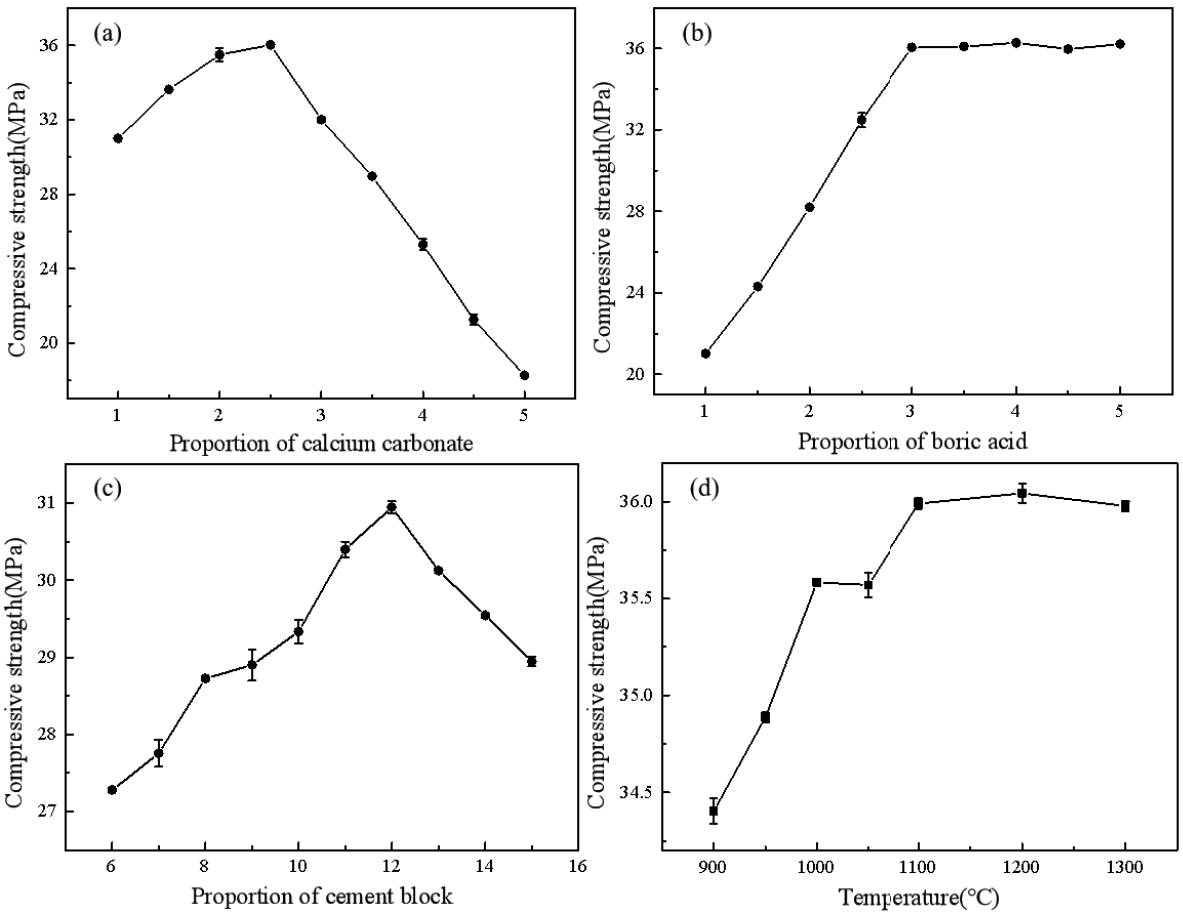

Fig. 3. Effect of raw material proportions and temperature on glass pumice compressive strength. (a–d represent calcium, boric acid, cement block and temperature respectively) (n = 3, $SD_{(a,b,c,d)}$ = 0.154, 0.082, 0.085, 0.038, respectively)

an important role in the formation of glass pumice's pore structure and affected the Pb^{2+} adsorption performance of glass pumice. During the process of calcination, $CaCO_3$ was decomposed into CaO and CO_2, which provided interspaces for the materials [23]. It was found that a high proportion of calcium carbonate caused the glass pumice out of shape while a low proportion of calcium carbonate caused the glass pumice porosity too small through its physical characterization. Therefore, the optimum calcium carbonate proportion of 2.5 was adopted.

3.1.2. Effect of boric acid proportion

As a melting aid, boric acid can improve the heat resistance and transparency of glass products, increase the compressive strength, and also shorten the melting time [24]. Fig. 3b shows that the proportion of boric acid had a significant effect on the compressive strength of glass pumice. With the increase of boric acid proportion, the compressive strength of glass pumice raised from 21 to 36 MPa, which reached the maximum when the proportion of boric acid was 3, and then a plateau was reached, the compressive strength of the glass pumice didn't improve obviously.

3.1.3. Effect of cement block powder

The addition of cement block powder was mainly to improve the compressive strength of the glass pumice. With the increase of cement block powder proportion, the compressive strength of the glass pumice presented a trend of

rising at the beginning, and then falling in Fig. 3c. According to its physical characteristics, it was found that the sample was in powder form when the cement block powder proportion was high, while the sample porosity was small when the cement block powder proportion was low, which did not meet the pore requirements of the adsorbent material. When the cement block powder proportion accounted for 12, the glass pumice was not only large in porosity but also had an optimum performance in compressive strength.

3.1.4. Effect of firing temperature

The firing temperature has a great influence on the glass pumice's compressive strength. The compressive strength of glass pumice showed a tendency to increase at the beginning and then to level off as the firing temperature increased in Fig. 3d. Moreover, when the temperature was low, the glass powder failed to melt, leading to a powdery sample. When the temperature reached 1,000°C, the sample was already molded, and the porosity was sufficient high enough for the adsorption. It can be found from Fig. 3d that the compressive strength didn't increase obviously from 1,000°C to 1,100°C. Because the metal compound in the cement block powder acted as a fluxing agent [25], the glass powder had completely melted at 1,000°C, so the increase of temperature has little effect on the results. Considering the heating time and cost, 1,000°C was adopted finally.

The glass pumice was successfully prepared according to the optimal raw material proportion and firing temperature, and its compressive strength was measured by manual compression testing machine. It was found that the compressive strength could reach 36.7 MPa, which was better than the high-strength lightweight aggregate ceramsite prepared by Liu et al. [26]. The basic strength requirements of the adsorbent were thus met.

3.2. Characteristics of glass pumice

3.2.1. Physical properties of glass pumice

The glass pumice samples are irregular block with off-white and particulate matter, and the glass pumice samples are rough and even with amounts of interstice. It was obviously found that the glass pumice contained different sizes of holes. The specific surface area of the material was measured by using specific surface aperture distribution. BET results showed that the specific surface areas of glass pumice, glass powder and cement block were 2.92, 1.68 and 1.98 $m^2\ g^{-1}$ respectively, the pore volumes were 0.0055, 0.0048 and 0.0015 $cm^3\ g^{-1}$ respectively, the pore diameters were 7.5, 11.8 and 7.5 nm. The existence of pores indicated that it was beneficial to the diffusion of Pb^{2+} to the surface and interior of the glass pumice. By comparing the physical properties of glass powder, cement block and glass pumice, it was obvious that the specific surface and pore volume of glass pumice had improved to a certain extent which indicated that the glass pumice was much beneficial to the further improvement of adsorption performance. EDS results are listed in Table 3, the W_t % represents the weight percentage, A_t % represents the atomic percentage. From the EDS results, we found that the glass pumice was rich in elements, the main element Si was very prominent, and it also contained mineral elements such as Na, Mg, Al, K, and Ca. We also carried out a leaching test on the glass pumice. The leaching concentration of heavy metals were all below the national limit (Pb 0.015 mg L^{-1}), and under the action of boric acid, the molten glass powder would form many glass grids, which could bind up heavy metals well. The heavy metals existed in the glass pumice were in a solid solution combined state, which was extremely stable.

3.2.2. SEM analysis of glass pumice

As shown in Fig. 4, three different surface morphologies were obtained by SEM analysis. From Fig. 4c it can be clearly observed that the surface of the glass pumice is much rougher and uneven compared with the cement block and glass powder. The wrinkles on the glass pumice surface in Fig. 4c indicate that there were many mesoporous in the glass pumice. It can be inferred that the existence of mesopores improved the transportation of metal ions in the heavy metal solution to the interior of the glass pumice. Pb^{2+} had more active sites in contact with the glass pumice surface, which was beneficial to the adsorption capacity of glass pumice to Pb^{2+}.

3.2.3. FTIR analysis of glass pumice

FTIR spectrum analysis of the glass pumice, cement block powder and glass powder are shown in Fig. 5. It was obviously observed that there were different FTIR spectra between them. The broad peak near 3,480 cm^{-1} was the stretching vibration peak of the Si–OH hydroxyl group, the broad peak near 1,612 cm^{-1} was the stretching vibration peak of the Si–Si hydroxyl group, the stretching vibration adsorption peak of the B–O bond was at 1,375 cm^{-1}, and the stretching vibration peak at 1,076.4 cm^{-1} was generated by the tensile vibration of the Si–O bond, and the vibration adsorption peak of Si–O–Si of inorganic minerals was at 797 cm^{-1} [27–29]. From the FTIR spectrum image, it can be seen that during the preparation process of glass pumice, B–O bonds were formed [30], which played a role in maintaining the stability of the foaming channel. The 3,480 cm^{-1} was related to Si–OH and smaller fluctuation of glass pumice compared with the cement block powder and glass powder. It indicated that Si–OH decreased after

Table 3
EDS element analysis of glass pumice

Element	CK	OK	NaK	MgK	AlK	SiK	KK	CaK
W_t %	4.98	36.41	4.01	1.02	1.26	32.01	1.11	19.2
A_t %	9.01	49.46	3.79	0.92	1.01	24.78	0.62	10.41

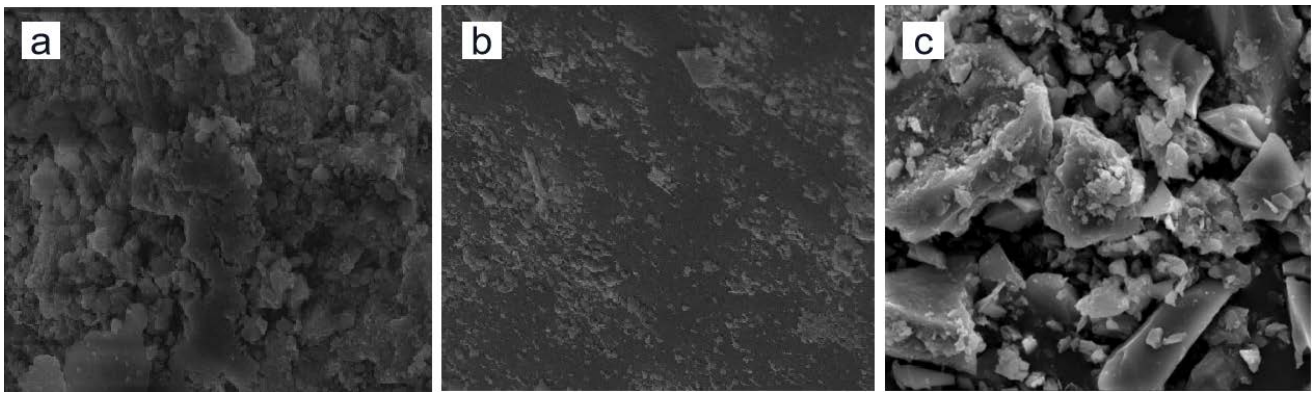

Fig. 4. SEM images of materials (a) cement block, (b) glass powder and (c) glass pumice.

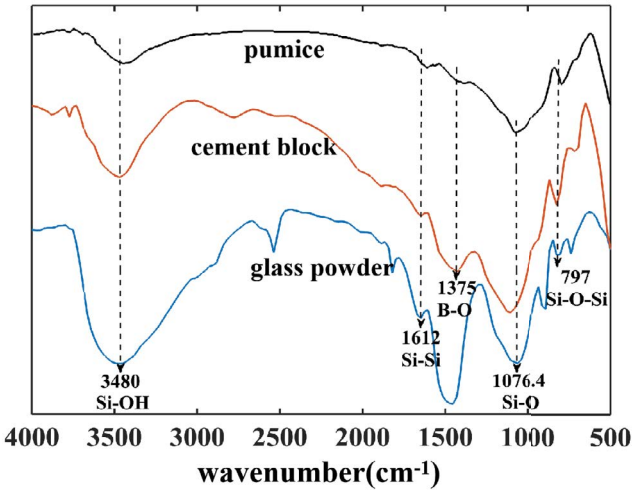

Fig. 5. FTIR analysis of glass pumice, cement block and glass powder.

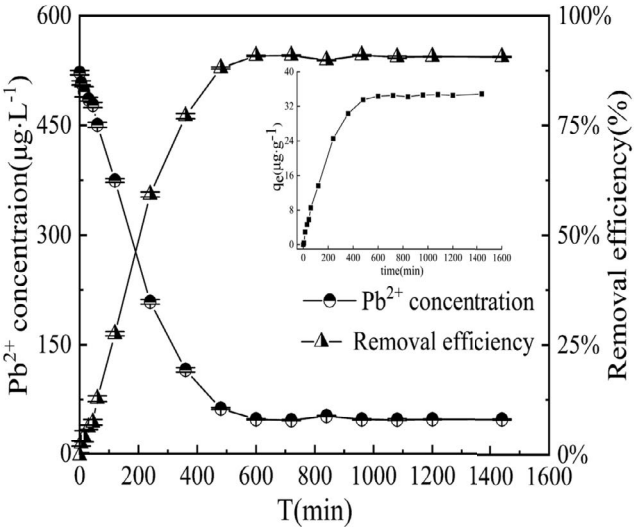

Fig. 6. Pb^{2+} adsorption by glass pumice.

preparation. Furthermore, the Si–O–Si stretching vibration peak indicated that Si in the pumice compared to glass powder and cement block powder, Si–O–Si bonds under the action of boric acid.

3.3. Pb^{2+} adsorption by glass pumice

Fig. 6 shows that the effect of contact time of Pb^{2+} adsorption by glass pumice. At the first 360 min, the concentration of Pb^{2+} declined from 520 to 112 μg L^{-1} rapidly. From the change of Pb^{2+} concentration, it can be seen that the adsorption equilibrium time was 600 min, while the maximum adsorption amount and removal efficiency from heavy metal solution by glass pumice were 34 μg g^{-1} and 90.96%. It was obvious that the Pb^{2+} concentration decreased significantly with the increase of contact time from 0 to 360 min. After increasing the contact time to 600 min, the adsorption capacity no longer fluctuated greatly and tended towards equilibrium. The faster adsorption rate in the initial stage of adsorption was because there were a large number of adsorption sites on the surface of the glass pumice. Moreover, the adsorption process was based on the Pb^{2+} gradient between the solid and liquid phases, with the adsorption at this stage belonged to surface adsorption [31]. As the adsorption sites gradually reach saturation, the adsorption rate depended on the speed of heavy metal ions entering the adsorbent from the outside to the inside. Moreover, high Pb^{2+} concentration caused a large driving force for mass transfer. Then the Pb^{2+} began to migrate and diffuse from the surface of the adsorbent to the inside of the adsorbent, and the adsorption rate becomes slower.

There were similar results with other adsorption materials for Pb^{2+} adsorption in the previous studies (Table 4). The adsorption trend was similar but the adsorption capacity was lower than other research. The reason for this phenomenon may be that many of the adsorbent materials studied were in powder form, while the adsorbent material in this study was lumpy, which had fewer adsorption sites and a smaller specific surface area, resulted in a smaller adsorption capacity. However, the adsorbent used in this study was construction waste, which was cheap and easy to obtain compared to synthetic adsorbents, thus achieved the purpose of using waste treat waste.

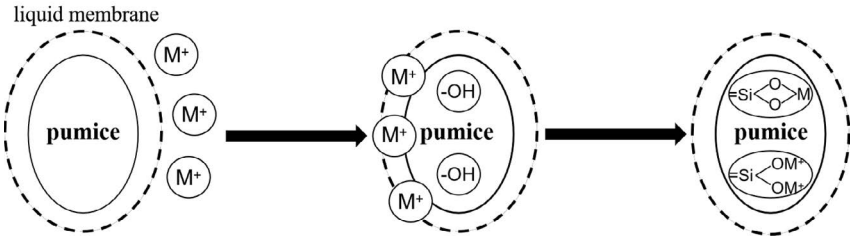

Fig. 7. Schematic representation for the Pb^{2+} adsorption process of glass pumice (M^+ represents heavy mental ions).

Table 4
Similar results about the Pb^{2+} adsorption of other materials

Adsorbent	Adsorption conditions	Adsorption capacity (mg g^{-1})	Equilibrium time	Reference
Alumina-coated carbon nanotube	C_0 = 20 mg L^{-1}, 25°C, pH = 7	14	60 min	Gupta et al. [32]
Activated carbon	C_0 = 60 mg L^{-1}, 25°C, pH = 4	52.54	60 min	Zhang and Tong [33]
Phanerochaete chrysosporium	C_0 = 48 mg L^{-1}, 28°C, pH = 4.5	27.49	720 min	Wu et al. [11]
Diatomite	C_0 = 50 mg L^{-1}, 15°C, pH = 5.4	17.45	5 min	Shen et al. [34]

3.4. Adsorption mechanism analysis

Schematic representation for the Pb^{2+} adsorption process of glass pumice was shown in Fig. 7, which can facilitate in explaining the adsorption internal process. The first step was the liquid membrane diffusion process, where there was a concentration difference between the glass pumice and the surrounding liquid film. Under the action of the heavy metal concentration gradient force, the heavy metal ions were quickly adsorbed, and then penetrated into the pores from the surface. The heavy metal ions inside the pores reacted with related substances on the inner surface of the glass pumice to generate new substances, thereby achieved the purpose of removing heavy metal ions. When heavy metal ions entered the pores of the adsorbent, the following reactions occurred:

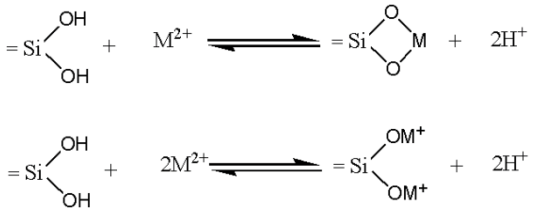

Besides, adsorption kinetics and isotherms analysis were conducted (Figs. 8 and 9), and the adsorption kinetics' non-linear fitting results and isotherm adsorption model non-linear fitting results were listed in Tables 5 and 6, respectively. The relevant constants were calculated by the model, and the credibility of each model can be judged by comparing the correlation coefficients (R^2).

3.4.1. Adsorption kinetics analysis

Adsorption kinetics is a critical method for investigating the mechanism of adsorption. It is necessary to know

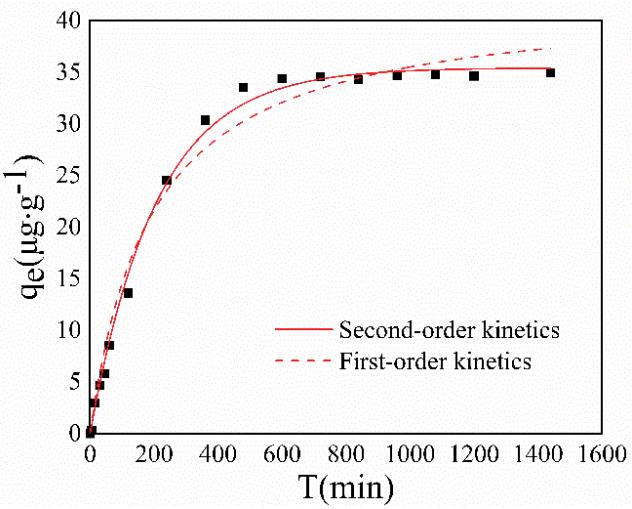

Fig. 8. Adsorption kinetics analysis.

the value of q_e for fitting the experimental data to Eq. (5) and Eq. (6). In order to understand the adsorption kinetics mechanism of Pb^{2+} by glass pumice, the first order kinetics and the second-order kinetics simulations of the adsorption process were carried out respectively. The kinetics model fitting results are shown in Fig. 8 and Table 5, it can be seen from Table 5 that two kinetics models could well fit the process of adsorbing Pb^{2+} by glass pumice. Although the first order and second-order kinetics showed a better result (R^2 = 0.976 and 0.996, respectively) for adsorbing Pb^{2+} by glass pumice, the second-order kinetics model was much more suitable for describing the adsorption process of Pb^{2+} compared to the first order kinetics model. This result agreed well with Yang's [35]. The adsorption process simulated by the second-order kinetics was a chemical

Table 5
Adsorption kinetics fitting results

First-order model			Second-order model		
q_e (μg g^{-1})	k_1 (min^{-1})	R^2	q_e (μg g^{-1})	k_2 (g(mg min)$^{-1}$)	R^2
35.43	0.0048	0.976	38.13	1.2375	0.996

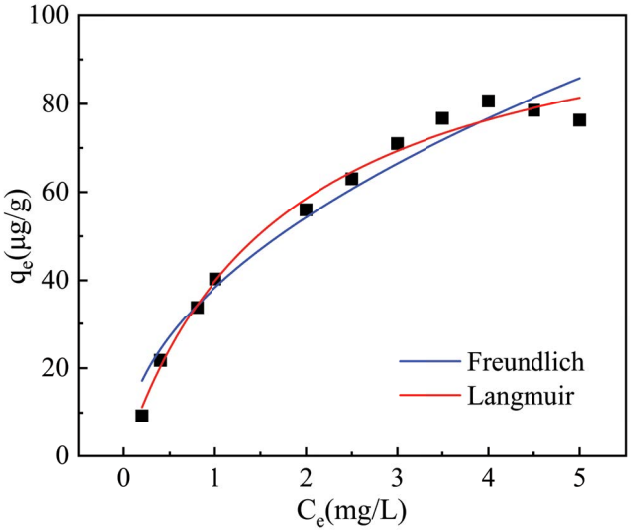

Fig. 9. Adsorption isotherms analysis.

adsorption process that included ions exchange between chemical bonds and the adsorption, which indicated that glass pumice and Pb^{2+} exchanged charge through the shared electron pair and the electrostatic gravity. Determining q_e accurately is a difficult task, because in many adsorbate-adsorbent interactions, the chemisorption becomes very slow after an initial fast response and it is difficult to ascertain whether equilibrium is reached or not. Furthermore, the second-order kinetic model can describe all the processes of chemical adsorption, including external liquid film diffusion, surface adsorption and internal diffusion, among others [36]. It can explain the adsorption mechanism of glass pumice on heavy metals ions comprehensively. Moreover, the first order model was only applicable to the kinetic description of the initial adsorption process, so it was not as accurate as the second-order kinetic equation, which could describe the entire progress of adsorption. Furthermore, one of the advantages of the second-order equation for estimating the q_e values is its small sensitivity for the influence of random experimental errors [37].

3.4.2. Adsorption isotherms analysis

The adsorption equilibrium isotherms were used to describe the adsorption process under equilibrium state. The Langmuir and Freundlich isotherm adsorption models were used to fit the experimental data of the Pb^{2+} adsorption by glass pumice. The adsorption isotherm of Pb^{2+} on glass pumice is shown in Fig. 9, and the fitting results of the adsorption isotherm model are listed in

Table 6
Isotherm adsorption model fitting results

Langmuir model			Freundlich model		
q_e (μg g^{-1})	k_1 (L mg^{-1})	R^2	n	K_F	R^2
36	0.544	0.986	0.122	0.447	0.957

Table 6. Comparing the two adsorption isotherm models, the adsorption of Pb^{2+} by glass pumice is in accordance with the Langmuir and Freundlich adsorption isotherms (because the two adsorption isotherm models both have a good linear relationship, R^2 are both greater than 0.95, the model is applicable in all of the cases with R^2 in the range of 0.940–0.999). It can be seen from Table 6 that the adsorption isotherms of Pb^{2+} on glass pumice was well fitted by the Langmuir isotherm adsorption model with R^2 = 0.986, which was better than Freundlich model (R^2 = 0.957). Since physical adsorption often occurs in multi-molecular layers, while chemical adsorption generates in monolayers, where the active sites were evenly distributed on the surface of the adsorbent, it can be inferred that the adsorption of Pb^{2+} on glass pumice is mainly monolayer and chemical adsorption. Further, the essential characteristics of the Langmuir isotherm can be described by the separation factor R_L and the calculate value was 0.3 ($0 < R_L < 1$), indicating that the adsorption process was easy to proceed [38]. It also showed that the maximum adsorption capacity of glass pumice was 36 μg g^{-1}. which was basically consistent with the data measured in the actual experiments. This phenomenon is derived from its assumption of heterogeneous adsorbent surface, whereas the surface of glass pumice is relatively uniform, with the results in agreement with Liu et al. [39]. It was further verified that the adsorption capacity of glass pumice for Pb^{2+} has a certain limit value, so the adsorption capacity will not change when the initial concentration of the solution reached a certain value [40].

4. Conclusions

This study successfully prepared a novel adsorbent, glass pumice, based on construction waste, and it was demonstrated that the glass pumice had effective adsorption performance through removing Pb^{2+} from heavy mental solution by various physical characterizations. The glass pumice's compressive strength was significantly affected by the proportion of calcium carbonate, boric acid and cement block powder, and the firing temperature. The glass pumice adsorption performance was obviously affected by the dosage of adsorbent. It was proved that the

second-order kinetic equation could better fit the kinetic process of Pb^{2+} adsorption by glass pumice. The adsorption model also conformed to the Langmuir isotherm model. The preparation of glass pumice provided an accessible possibility research idea for the production of environmentally friendly adsorbents and the removal of heavy metal ions.

Acknowledgments

This work was supported by the National Natural Science Foundation of China (51002196), and the Jiangsu Province Graduate Practice Innovation Program Project (SJCX20_0305).

Disclosure statement

No potential conflict of interest was reported by the authors.

References

[1] D. Ko, P.D. Mines, M.H. Jakobsen, C.T. Yavuz, H.C.B. Hansen, H.R. Andersen, Disulfide polymer grafted porous carbon composites for heavy metal removal from stormwater runoff, Chem. Eng. J., 348 (2018) 685–692.
[2] L.D. Sabin, J.H. Lim, K.D. Stolzenbach, K.C. Schiff, Contribution of trace metals from atmospheric deposition to stormwater runoff in a small impervious urban catchment, Water Res., 39 (2005) 3929–3937.
[3] F. Clauson-Kaas, C. Ramwell, H.C.B. Hansen, B.W. Strobel, Ptaquiloside from bracken in stream water at base flow and during storm events, Water Res., 106 (2016) 155–162.
[4] C.S. Nkutha, N.D. Shooto, E.B. Naidoo, Adsorption of Cr(VI), Pb(II) ions and methylene blue dye from aqueous solution using pristine and modified coral limestone, Asian. J. Chem., 32 (2020) 2624–2632.
[5] Y. Wang, Recent progress of the treatment of heavy metal wastewater, Shanxi. Archit., 42 (2016) 189–190.
[6] S. Li, H. Zha, Z. Fan, Research status and prospects in treatment technique for Pb^{2+}-containing wastewater, Chem. Ind. Eng. Process., 30 (2011) 336–340.
[7] H. Qian, Z.H. Fu, S. Chen, Q. Zhou, Z.Y. Lian, W.J. Wei, H. Lu, Adsorption behavior of PP-g-GMA-DETA chelating fiber on Pb^{2+}, Ind. Water. Treat., 39 (2019) 71–75.
[8] B.J. Glaister, T.D. Fletcher, P.L.M. Cook, B.E. Hatt, Interactions between design, plant growth and the treatment performance of stormwater biofilters, Ecol. Eng., 105 (2017) 21–31.
[9] M. Sekar, V. Sakthi, S. Rengaraj, Kinetics and equilibrium adsorption study of lead(II) onto activated carbon prepared from coconut shell, J. Colloid Interface Sci., 279 (2004) 307–313.
[10] H. Faghihian, M.G. Marageh, H. Kazemian, The use of clinoptilolite and its sodium form for removal of radioactive cesium, and strontium from nuclear wastewater and Pb^{2+}, Ni^{2+}, Cd^{2+}, Ba^{2+} from municipal wastewater, Appl. Radiat. Isot., 50 (1999) 655–660.
[11] J. Wu, Q.B. Li, Study on mechanism of lead biosorption by *Phanerochaete chrysosporium*, Acta Sci. Circumst., 3 (2001) 291–295.
[12] K.R. Zhu, H. Fu, J.H. Zhang, X.S. Lv, J. Tang, X.H. Xu, Studies on removal of NH_4^+–N from aqueous solution by using the activated carbons derived from rice husk, Biomass Bioenergy, 43 (2012) 18–25.
[13] H. Zheng, L.J. Han, H.W. Ma, Y. Zheng, H.M. Zhang, D.H. Liu, S.P. Liang, Adsorption characteristics of ammonium ion by zeolite 13X, J. Hazard. Mater., 158 (2008) 577–584.
[14] S.Z. Zhang, Present situation and countermeasures of resource utilization of construction waste, Const. Sci. Tech., 388 (2019) 91–93.
[15] S. Omary, E. Ghorbel, G. Wardeh, Relationships between recycled concrete aggregates characteristics and recycled aggregates concretes properties, Constr. Build. Mater., 108 (2016) 163–174.
[16] R. Han, Study on the problems and countermeasures of Jinan construction waste recycling, Energy Conserv. Environ. Prot., 3 (2020) 34–35.
[17] Z.M. Wu, K. Bao, J. Cao, X.F. Yan, H.H. Zhang, Analysis on the current situation of domestic waste treatment technology in China and discussion on management countermeasures, Energy Conserv. Environ. Prot., 11 (2019) 37–38.
[18] Y.L. Qi, L.B. Hao, J. Zhou, Analysis of a new recycling treatment technology which uses waste glass-green light stone material production, Guangdong. Chem. Ind., 4 (2018) 108–110.
[19] Q. Gu, S. Shu, Y. Ke, Z.N. Zhou, N. Liu, Experimental study on mechanical performance and insulation property of glass pumice concrete, J. Wuhan Univ. Technol., 2 (2015) 92–95.
[20] M. Yurtsever, I.A. Sengil, Biosorption of Pb(II) ions by modified quebracho tannin resin, J. Hazard. Mater., 163 (2019) 58–64.
[21] X. Guo, J.L. Wang, Comparison of linearization methods for modeling the Langmuir adsorption isotherm, J. Mol. Liq., 296 (2019) 111850, doi: 10.1016/j.molliq.2019.111850.
[22] R. Karthik, S. Meenakshi, Biosorption of Pb(II) and Cd(II) ions from aqueous solution using polyaniline/chitin composite, Sep. Sci. Technol., 51 (2016) 733–742.
[23] X.P. Zeng, B. Wu, S. Jiang, X.R. Deng, The analysis for the calcium carbonate at high temperatures, Guangdong Chem. Ind., 37 (2010) 70–72.
[24] J.B. Wang, K. Li, S.J. Huang, J.Z. Xiao, F. Xia, Influence of the boric acid on sintering and crystallization behavior of the fused silica, Bull. Chin. Ceram. Soc., 28 (2009) 1107–1111.
[25] F. Xi, D.C. Zhao, Preparation of ultra-lightweight fly ash ceramic (ULFAC), investigation and application of the bloating mechanism, J. Funct. Mater., 41 (2010) 518–523.
[26] X. Liu, T. Wu, X. Yang, H. Wei, P.Z. Li, Mechanical properties and microstructure of fiber reinforced high strength lightweight aggregate concrete, J. Build Mater., 22 (2019) 700–706+713.
[27] L. Kou, C. Gao, Making silica nanoparticle-covered graphene oxide nanohybrids as general building blocks for large-area superhydrophilic coatings, Nanoscale, 3 (2010) 519–528.
[28] Q. Liu, J.B. Shi, J.T. Sun, T. Wang, G.B. Jiang, Graphene and graphene oxide sheets supported on silica as versatile and high-performance adsorbents for solid-phase extraction, Angew. Chem. Int. Ed., 50 (2011) 5913–5917.
[29] Y.K. Yang, S.Q. Qiu, W. Cui, Q. Zhao, X.J. Cheng, R.K.Y. Li, X.L. Xie, Y.W. Mai, A facile method to fabricate silica-coated carbon nanotubes and silica nanotubes from carbon nanotubes templates, J. Mater. Sci., 44 (2009) 4539–4545.
[30] B.B. Wang, H.D. Zhu, J. Chen, Study on microwave vitrification technology of heavy metal contaminated soil, Environ. Eng., 31 (2013) 96–98+108.
[31] B. Wang, W.F. Zhu, L.J. Wang, P. Peng, J.M. Zeng, Preparation of sintering-expanded haydite based on Guangxi pingguo red mud and adsorption of Pb^{2+} in water, J. Wuhan Univ. Technol., 36 (2014) 30–34.
[32] V.K. Gupta, S. Agarwal, T.A. Saleh, Synthesis and characterization of alumina-coated carbon nanotubes and their application for lead removal, J. Hazard. Mater., 185 (2011) 17–23.
[33] S.Q. Zhang, S.T. Tong, The adsorption studies of activated carbon for heavy metal ions of lead, cadmium and copper, Environ. Sci. Manage., 33 (2008) 91–94.
[34] Y.B. Shen, Y.M. Zhu, Z.A. Wang, D.Z. Wei, Adsorption of Pb^{2+} in hydrofacies by diatomite, J. Northeast. Univ., 24 (2003) 982–985.
[35] L.Q. Yang, S.R. Zhang, Y.X. Peng, G.Y. Wang, X.X. Xu, Adsorption characteristics of Cd^{2+} and Pb^{2+} in wastewater by 4 agricultural wastes, J. Ecol. Rural. Environ., 36 (2020) 1468–1476.
[36] Z.L. Zhou, W.L. Wu, Y. Li, H.W. Sun, Sorption and desorption behaviors of three PAHs by charcoals, J. Agro-Environ. Sci., 27 (2009) 813–819.
[37] S.S. Gupta, K.G. Bhattacharyya, Kinetics of adsorption of metal ions on inorganic materials: a review, Adv. Colloid Interface Sci., 162 (2011) 39–58.

[38] N. Kannan, M.M. Sundaram, Kinetics and mechanism of removal of methylene blue by adsorption on various carbons-a comparative study, Dyes Pigm., 51 (2001) 25–40.
[39] Q.S. Liu, Z. Tong, P. Wang, J.P. Jiang, N. Li, Adsorption isotherm, kinetic and mechanism studies of some substituted phenols on activated carbon fibers, Chem. Eng. J., 157 (2010) 348–356.
[40] T. Qiu, Y. Zeng, C.S. Ye, H. Tian, Adsorption thermodynamics and kinetics of p-Xylene on activated carbon, J. Chem. Eng. Data, 57 (2012) 1551–1556.